

---

# Calculation of photonic band structures for 1D quasicrystals and 2D square crystals

Master's Thesis in Physics

Presented by

**Yang Kuang**

April 18, 2018

Institut für Theoretische Physik

Friedrich-Alexander-Universität Erlangen-Nürnberg



Supervisor: Prof. Dr. Michael Schmiedeberg

## Declaration of Authorship

I confirm that this Master's thesis is my own work and that I have not used any sources other than those listed in the bibliography and identified as references. I have not submitted this thesis at any other institution in order to obtain a degree.

Place and date:

---

Signature:

---

# Contents

<b>Declaration of Authorship</b>	<b>iii</b>
<b>1 Introduction</b>	<b>1</b>
1.1 Photonic crystal . . . . .	1
1.2 Brief introduction of quasicrystals . . . . .	3
1.3 Construction of quasicrystals . . . . .	4
1.4 The cut and project method . . . . .	5
1.5 Photonic quasicrystal . . . . .	5
<b>2 Theoretical background</b>	<b>7</b>
2.1 Maxwell equations in dielectric materials . . . . .	7
2.2 Master equation in dielectric material . . . . .	10
2.3 Eigenvalue equations in photonic crystal . . . . .	10
2.4 Master equation in photonic quasicrystal . . . . .	13
2.5 Eigenvalue equation for 1-dimensional quasicrystal . . . . .	15
<b>3 Method for numerical calculation of the band structure of a one dimensional photonic quasicrystal</b>	<b>19</b>
<b>4 Results and discussion</b>	<b>25</b>
4.1 Band structures of two dimensional square photonic crystals . . . . .	25
4.2 Band structures of one dimensional Fibonacci-like photonic quasicrystals	29
<b>5 Summary and Outlook</b>	<b>35</b>
5.1 Summary of results . . . . .	35
5.2 Outlook . . . . .	36
<b>Bibliography</b>	<b>37</b>

## Chapter 1

# Introduction

The topic of this thesis is the discussion of the calculation of a photonic band structure of a quasicrystal. Furthermore, we will carry out the calculation of the photonic band structures of one dimensional Fibonacci-like quasicrystalline dielectric materials (i.e. photonic quasicrystal) and two dimensional periodic square crystal from which the structure of the former can be generated through cut and project method.

### 1.1 Photonic crystal

Before dealing with the concept of photonic quasicrystal, it is necessary to introduce the materials, which are named photonic crystals, in the first place. Photonic crystals are periodic optical nano-structures that can affect electromagnetic waves which travel in them. Figure 1.1 shows a two dimensional photonic crystal.

Aiming at diminishing the spontaneous emission in the propagation of electromagnetic waves in material, E.Yablonytch raised the idea that one can construct periodic

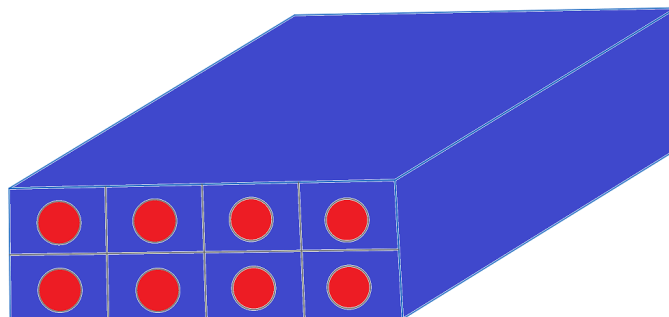


FIGURE 1.1: A two dimensional photonic crystal with periodic square lattice. In each cell there is a cylinder dielectric material with different permittivity or air

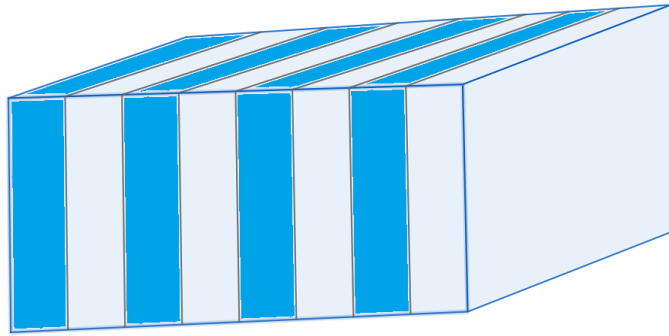


FIGURE 1.2: One dimensional periodic multilayer dielectric stacks

dielectric materials which can forbid propagation of light with certain frequencies due to the existence of band gaps in the photonic band structure or dispersion curves ( $\omega \sim k$ ) (Yablonovitch and Eli, 1987)

The earliest example of photonic bandgap was already found in 1887 by English physicist Lord Rayleigh (Rayleigh, 1888), who was able to observe photonic band gap in one dimensional periodic multilayer dielectric stacks, which is shown in Figure 1.2. The mechanism of the occurring of photonic band structure is similar to that of electronic band structure due to the comparability of solving the Schrödinger equation and the Maxwell equations in periodic materials (Joannopoulos, 2008), the latter of which describes the allowed bands and forbidden bands of the electron energy. In principal photonic crystals are used to manipulate light and are applied in many fields. It is easy to figure out that there are three branches of photonic crystals: one-dimensional, two-dimensional and three-dimensional photonic crystals, according to how many dimensions does it need to describe their geometric structures. Each of them has its own use or the potential of being used in individual fields. For example one dimensionally, the thin-film optics, which deals with thin layers of various materials (Knittl, 1976), can be used to create optical coatings such as low emissivity panes of glass and high precision optical filters and mirrors and so on. Two-dimensional photonic crystal fibers (Russell, 2003) are applicable in nonlinear devices and guiding exotic wavelengths. While three-dimensional photonic crystals have the potential to play a crucial role in optical computers (Hwang, Lee, and Kim, 2013).

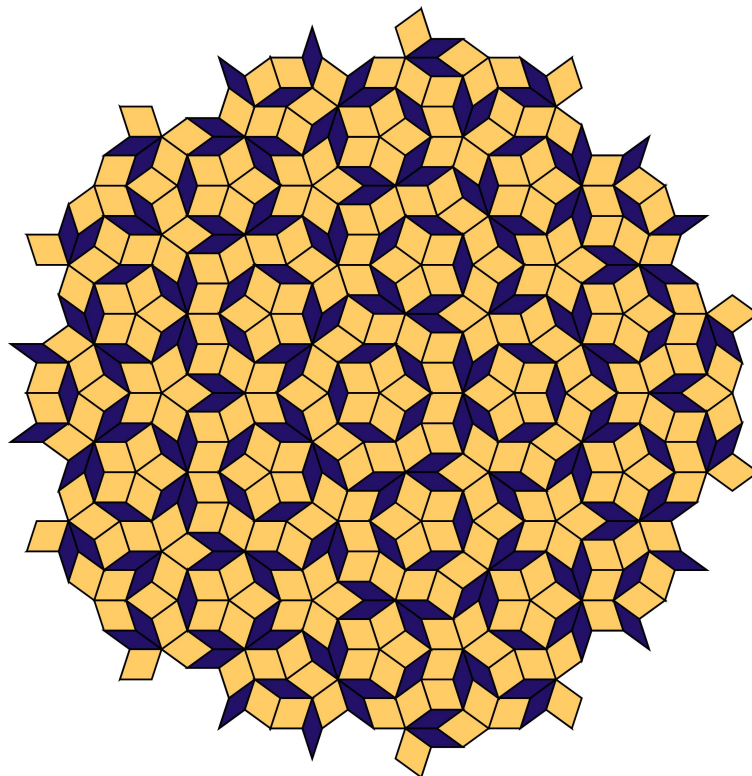


FIGURE 1.3: Two dimensional Penrose tiling

## 1.2 Brief introduction of quasicrystals

Quasicrystals are solids of which the building blocks can fill the entire space densely and the structure is ordered but does not possess translational symmetry in  $n$  directions if the dimension of the space is  $n$ , while it can have translational symmetry in certain  $m$  directions while  $m$  is smaller than  $n$ , e.g.  $m=n-1$ . We know that the crystallographic restriction theorem requires that crystals can only have 2, 3, 4 or 6-fold rotational symmetries (Senechal, 1995). By contrast, quasicrystals have other possibilities of rotational symmetries such as 5, 8 and 12-fold symmetries. Figure 1.3 shows a widely known example of quasicrystal, the two dimensional Penrose tiling.

Quasicrystals are not like amorphous solids because their structures show well-defined discrete point group symmetries (Levitov and Rhyner, 1988), which is similar to crystals. With respect to the translational symmetry of crystals, quasicrystals possess another kind of translational order known as quasiperiodicity. Actually quasicrystals are a special case of more general quasiperiodic patterns. (Kraus and Zilberberg, 2016) Any finite piece in a quasiperiodic pattern is unique while there are infinite many pieces that are almost like it. Although aperiodic tilings have already been

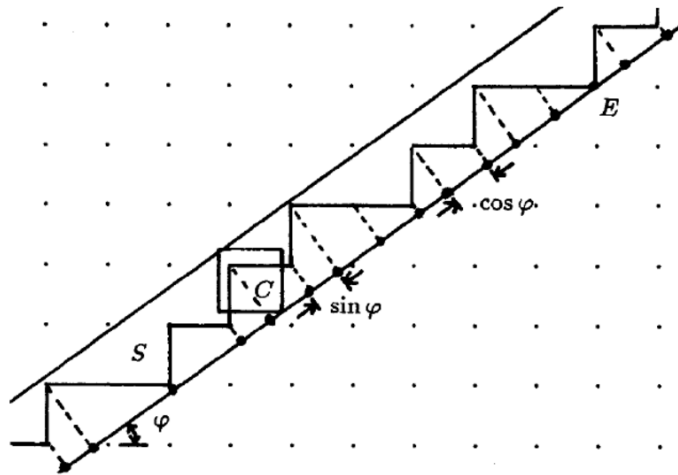


FIGURE 1.4: The cut and project method used to generate one dimensional quasicrystal from two dimensional periodic lattice. This figure is taken from Albertus Hof. Quasicrystals, aperiodicity and lattice systems. PhD thesis, University of Groningen

studied in the 1960s, only since the 1980s did quasicrystals receive much attention by academic community. Dan Shechtman is the first to have discovered quasicrystal (Shechtman et al., 1984), and received Nobel Prize in Chemistry in 2011.

### 1.3 Construction of quasicrystals

Mathematically there are several different approaches to construct quasicrystalline patterns. Among them, there is the algebraic theory called the grid method developed by de Bruijn (De Bruijn, 1981), which has been used to construct the 2-dimensional Penrose tiling. The 3-dimensional generalization of the grid method was first discussed by Mackay (Mackay, 1982) and later theoretically described by Kramer and Neri (Kramer, Neri, and IUCr, 1984). On the other hand, there is an equivalent approach to construct the quasilattice, the so called cut and projection method, which are presented concurrently by Elser (Elser, 1985), Duneau and Katz (Duneau and Katz, 1985). The cut and projection approach is also the method that will be used in this thesis.

## 1.4 The cut and project method

De Wolff is one of the first to have studied higher dimensional crystallography (Wolf and Aalst, 1972). According to his work, quasicrystalline structure can be obtained through irrational cutting from higher dimensional superspace, which is periodic, comparing with the quasiperiodicity of the obtained quasicrystal in real space.

Figure 1.4 below depicts how the 1D Fibonacci chain is generated from a 2D periodic square lattice through the cut and projection method. In the figure the angle between the lattice and the projection line is required to be such that the tangent of which is irrational, for instance the golden ratio. (the obtained 1D structure should be called Fibonacci-like chain if the ratio is not golden ratio) As another example, the famous two dimensional Penrose tiling can also be generated through cut and project method applied on 5 dimensional periodic lattice (De Bruijn, 1981). As for the Penrose tiling, it has been proven that the grid method and the cut and projection method are equivalent (Gahler and Rhyner, 1986).

## 1.5 Photonic quasicrystal

It was found that two dimensional quasiperiodic structures with 8, 10 and 12 fold orientational symmetries can result in more isotropic photonic band structures with respect to normal periodic two dimensional photonic crystals (Rostami and Matloub, 2009). For the quasicrystalline case the width of the band gaps are nearly independent of the light propagation directions, which will make the confinement of light more easily (Wang et al., 2003). Thus it is interesting to study the photonic bandstructure of quasicrystals in addition to conventional photonic crystals.



## Chapter 2

# Theoretical background

In this chapter the equations needed to calculate the photonic band structures for periodic and quasiperiodic dielectric materials are deduced on the basis of Maxwell equations.

### 2.1 Maxwell equations in dielectric materials

Maxwell equations (Jackson, 1999) in matter, or so called "Macroscopic Maxwell equations", which decide how the electromagnetic field will behave in matter, are listed below in Gaussian units:

$$\nabla \cdot \mathbf{D} = 4\pi\rho \quad (2.1)$$

$$\nabla \cdot \mathbf{B} = 0 \quad (2.2)$$

$$\nabla \times \mathbf{E} = -\frac{1}{c} \frac{\partial \mathbf{B}}{\partial t} \quad (2.3)$$

$$\nabla \times \mathbf{H} = \frac{1}{c} \frac{\partial \mathbf{D}}{\partial t} + \frac{4\pi}{c} \mathbf{J} \quad (2.4)$$

where there are four fields appearing: the electric displacement field  $\mathbf{D}$ , the magnetic flux density  $\mathbf{B}$ , the electric field  $\mathbf{E}$  and the magnetic field strength  $\mathbf{H}$ .  $\rho$  stands for the free electric charge density and  $\mathbf{J}$  stands for the free electric current density, while  $c$  is the speed of light.

In dielectric materials, there are several assumptions (Joannopoulos, 2008) required to be made, which are needed to simplify the maxwell equations. Firstly, it is assumed that there is no free charge density and electric current density, which means that  $\rho = 0$  and  $\mathbf{J} = 0$  in the dielectric material.

The electric displacement field  $\mathbf{D}$  is defined as:

$$\mathbf{D} = \epsilon_0 \mathbf{E} + \mathbf{P} \quad (2.5)$$

where  $\mathbf{P}$  is the polarization density. In isotropic dielectric material we have

$$\mathbf{P} = \epsilon_0 \chi \mathbf{E} \quad (2.6)$$

where  $\chi$ , named the electric susceptibility is a function of position in the dielectric material if it is not homogeneous. So we have:

$$\mathbf{D} = \epsilon_0(1 + \chi)\mathbf{E} = \epsilon \mathbf{E} \quad (2.7)$$

$\epsilon$ , the permittivity is also a function of position:

$$\mathbf{D} = \epsilon(\mathbf{r})\mathbf{E} \quad (2.8)$$

The magnetic flux density  $\mathbf{B}$  and the magnetic field strength  $\mathbf{H}$  has the relation:

$$\mathbf{B} = \mu \mathbf{H} \quad (2.9)$$

where  $\mu$  is the permeability, which is approximately 1 in most dielectric materials. So it is assumed that:

$$\mathbf{B} = \mathbf{H} \quad (2.10)$$

With the assumptions above we now have a new set of simplified Maxwell equations:

$$\nabla \cdot (\epsilon \mathbf{E}) = 0 \quad (2.11)$$

$$\nabla \cdot \mathbf{B} = 0 \quad (2.12)$$

$$\nabla \times \mathbf{E} = -\frac{1}{c} \frac{\partial \mathbf{H}}{\partial t} \quad (2.13)$$

$$\nabla \times \mathbf{H} = \frac{\epsilon}{c} \frac{\partial \mathbf{E}}{\partial t} \quad (2.14)$$

## 2.2 Master equation in dielectric material

From (2.14) we have

$$\nabla \times \left( \frac{1}{\epsilon} \nabla \times \mathbf{H} \right) = \nabla \times \frac{1}{c} \frac{\partial \mathbf{E}}{\partial t} = \frac{1}{c} \frac{\partial}{\partial t} (\nabla \times \mathbf{E}) = -\frac{1}{c^2} \frac{\partial^2 \mathbf{H}}{\partial t^2} \quad (2.15)$$

Assuming that electric field and magnetic field can be written as product as positional dependent part and harmonic time dependent part (Joannopoulos, 2008):

$$\mathbf{E}(\mathbf{r}, t) = \mathbf{E}(\mathbf{r}) e^{i\omega t} \quad (2.16)$$

$$\mathbf{H}(\mathbf{r}, t) = \mathbf{H}(\mathbf{r}) e^{i\omega t} \quad (2.17)$$

After plugging (2.17) into (2.15) we will obtain

$$\nabla \times \left( \frac{1}{\epsilon} \nabla \times \mathbf{H}(\mathbf{r}) \right) = \frac{\omega^2}{c^2} \mathbf{H}(\mathbf{r}) \quad (2.18)$$

named the master equation (of magnetic field).

(2.18) is an ordinary eigenvalue problem, which is much easier to solve comparing with the master equation of electric field.

## 2.3 Eigenvalue equations in photonic crystal

Without losing generality, we consider the three dimensional periodic photonic crystal, which means that the permittivity is three dimensional periodic:

$$\epsilon(\mathbf{r}) = \epsilon(\mathbf{r} + \mathbf{T}) \quad (2.19)$$

where  $\mathbf{T}$  is any 3 dimensional lattice vector. Due to the Bloch theorem  $\mathbf{H}$  can be written in the following form:

$$\mathbf{H}(\mathbf{r}) = \mathbf{h}(\mathbf{r}) e^{i\mathbf{k} \cdot \mathbf{r}} \quad (2.20)$$

where  $\mathbf{h}(\mathbf{r})$  possess the same periodicity with  $\epsilon(\mathbf{r})$ . Because of the periodicity, both  $\epsilon(\mathbf{r})$  and  $\mathbf{h}(\mathbf{r})$  can be expanded as three dimensional Fourier series:

$$\mathbf{h}(\mathbf{r}) = \sum_{\mathbf{G}} \mathbf{h}_{\mathbf{G}} e^{i\mathbf{G}\cdot\mathbf{r}} \quad (2.21)$$

$$\frac{1}{\epsilon(\mathbf{r})} = \lambda(\mathbf{r}) = \sum_{\mathbf{G}} \lambda_{\mathbf{G}} e^{i\mathbf{G}\cdot\mathbf{r}} \quad (2.22)$$

where  $\lambda$  the reciprocal of  $\epsilon$  is expanded instead for conveniency.

inserting equations (2.21) and (2.22) into the master equation (2.18) gives:

$$\sum_{\mathbf{G}'} \sum_{\mathbf{G}} \nabla \times (\lambda_{\mathbf{G}'} e^{i\mathbf{G}'\cdot\mathbf{r}} \nabla \times (\mathbf{h}_{\mathbf{G}} e^{i((\mathbf{k}+\mathbf{G})\cdot\mathbf{r})})) = \frac{\omega^2}{c^2} \sum_{\mathbf{G}} \tilde{\mathbf{h}}_{\mathbf{G}} e^{i(\mathbf{k}_z+\mathbf{G})\cdot\mathbf{r}} \quad (2.23)$$

noting that we have:

$$(\nabla \times (\mathbf{a}A(\mathbf{r})))_i = \epsilon_{ijk} \partial_j (\mathbf{a}_k A) = \epsilon_{ijk} \mathbf{a}_k \partial_j A \quad (2.24)$$

where  $\mathbf{a}$  is any constant vector while A is any scalar function of position  $\mathbf{r}$  thus

$$(\nabla \times (\mathbf{h}_{\mathbf{G}} e^{i((\mathbf{k}+\mathbf{G})\cdot\mathbf{r})}))_i = \epsilon_{ijk} \partial_j e^{i((\mathbf{k}+\mathbf{G})\cdot\mathbf{r})} h_{\mathbf{G}k} = \epsilon_{ijk} (k_j + G_j) h_{\mathbf{G}k} e^{i((\mathbf{k}+\mathbf{G})\cdot\mathbf{r})} \quad (2.25)$$

In vector form we have then

$$\nabla \times (\mathbf{h}_{\mathbf{G}} e^{i((\mathbf{k}+\mathbf{G})\cdot\mathbf{r})}) = i((\mathbf{k} + \mathbf{G}) \times \mathbf{h}_{\mathbf{G}}) e^{i((\mathbf{k}+\mathbf{G})\cdot\mathbf{r})} \quad (2.26)$$

so

$$\nabla \times (\lambda_{\mathbf{G}'} e^{i\mathbf{G}'\cdot\mathbf{r}} \nabla \times (\mathbf{h}_{\mathbf{G}} e^{i((\mathbf{k}+\mathbf{G})\cdot\mathbf{r})})) = i\lambda_{\mathbf{G}'} \nabla \times ((\mathbf{k} + \mathbf{G}) \times \mathbf{h}_{\mathbf{G}}) e^{i((\mathbf{k}+\mathbf{G})\cdot\mathbf{r})} = \quad (2.27)$$

which also has the structure with (2.24), therefore:

$$\nabla \times (\lambda_{\mathbf{G}'} e^{i\mathbf{G}'\cdot\mathbf{r}} \nabla \times (\mathbf{h}_{\mathbf{G}} e^{i((\mathbf{k}+\mathbf{G})\cdot\mathbf{r})})) = -\lambda_{\mathbf{G}'} ((\mathbf{k} + \mathbf{G} + \mathbf{G}') \times ((\mathbf{k} + \mathbf{G}) \times \mathbf{h}_{\mathbf{G}})) e^{i((\mathbf{k}+\mathbf{G})\cdot\mathbf{r})} \quad (2.28)$$

In order to simplify the equation, considering the vector identical equation

$$\mathbf{A} \times (\mathbf{B} \times \mathbf{C}) = (\mathbf{A} \cdot \mathbf{C})\mathbf{B} - (\mathbf{A} \cdot \mathbf{B})\mathbf{C} \quad (2.29)$$

thus

$$((\mathbf{k} + \mathbf{G} + \mathbf{G}')) \times (((\mathbf{k} + \mathbf{G})) \times \mathbf{h}_{\mathbf{G}}) = (\mathbf{k} + \mathbf{G} + \mathbf{G}') \cdot \mathbf{h}_{\mathbf{G}} (\mathbf{k} + \mathbf{G}) - (\mathbf{k} + \mathbf{G} + \mathbf{G}') \cdot (\mathbf{k} + \mathbf{G}) \mathbf{h}_{\mathbf{G}} \quad (2.30)$$

According to the Maxwell equation of magnetic field in dielectric material

$$\nabla \cdot \mathbf{H} = 0 \quad (2.31)$$

where  $\mathbf{H}(\mathbf{r}, t) = \mathbf{H}(\mathbf{r})e^{i\omega t}$ . Therefore:

$$\nabla \cdot \mathbf{H} = \nabla \cdot \sum_{\mathbf{G}} \mathbf{h}_{\mathbf{G}} e^{i(\mathbf{G}+\mathbf{k})\cdot\mathbf{r}} e^{i\omega t} = \sum_{\mathbf{G}} i(\mathbf{k} + \mathbf{G}) \cdot \mathbf{h}_{\mathbf{G}} e^{i(\mathbf{G}+\mathbf{k})\cdot\mathbf{r}} e^{i\omega t} = 0 \quad (2.32)$$

hence we have for any  $\mathbf{k}$  and  $\mathbf{G}$

$$(\mathbf{k} + \mathbf{G}) \cdot \mathbf{h}_{\mathbf{G}} = 0 \quad (2.33)$$

as the result of this (2.30) can be further simplified:

$$((\mathbf{k} + \mathbf{G} + \mathbf{G}')) \times (((\mathbf{k} + \mathbf{G})) \times \mathbf{h}_{\mathbf{G}}) = -(\mathbf{k} + \mathbf{G} + \mathbf{G}') \cdot (\mathbf{k} + \mathbf{G}) \mathbf{h}_{\mathbf{G}} \quad (2.34)$$

substituting  $\mathbf{G} + \mathbf{G}'$  with  $\mathbf{G}'$  and applying the results above to equation (2.23) we finally obtained

$$\sum_{\mathbf{G}'} \lambda_{\mathbf{G}-\mathbf{G}'} (\mathbf{k} + \mathbf{G}) \cdot (\mathbf{k} + \mathbf{G}') \mathbf{h}_{\mathbf{G}'} = \left(\frac{\omega^2}{c^2}\right) \mathbf{h}_{\mathbf{G}} \quad (2.35)$$

This equation (2.35) is an eigenvalue problem. It should be mentioned that the eigenvalues  $\frac{\omega^2}{c^2}$  are functions of  $\mathbf{k}$ , which means that the relation in between describes exactly the photonic bandstructure of the one dimensional quasicrystal. By solving this matrix equation for photonic crystal, the corresponding photonic band structure ( $\omega \sim \mathbf{k}$ ) can then be calculated.

## 2.4 Master equation in photonic quasicrystal

As mentioned earlier in this thesis, we know that quasiperiodic structures can be obtained through irrational cutting from higher dimensional hypercubic lattice. This means that instead of studying materials whose permittivities are quasiperiodic directly, we could instead study its corresponding higher dimensional structures with permittivities possessing higher dimensional periodicity (Rodriguez et al., 2008).

Assume that we have 3 physical dimensions in the real space  $E^3$  and  $n$  total dimensions in the corresponding superspace  $E^n$ . The coordinates of the physical dimensions are denoted as  $\mathbf{x}$ , the total coordinates are denoted  $\mathbf{z}$ , while the coordinates of the orthogonal complementary space are denoted  $\mathbf{y}$ . We have in the physical space the original master equation:

$$\nabla \times \left( \frac{1}{\epsilon(\mathbf{x})} \nabla \times \mathbf{H}(\mathbf{x}) \right) = \left( \frac{\omega}{c} \right)^2 \mathbf{H}(\mathbf{x}) \quad (2.36)$$

This can be extended to  $E^n$ , where we replace  $\epsilon(\mathbf{x})$  with  $\tilde{\epsilon}(\mathbf{z})$  and  $\mathbf{H}(\mathbf{x})$  with  $\tilde{\mathbf{H}}(\mathbf{z})$ . Meanwhile, the nabla operator is unchanged, which still takes the derivative with respect to the  $\mathbf{x}$  coordinates. The new "permittivity" and "magnetic field strength" have to fulfill the following requirements:

$$\tilde{\epsilon}(\mathbf{z}) \big|_{\mathbf{y}=\mathbf{0}} = \epsilon(\mathbf{x}) \quad (2.37)$$

and

$$\tilde{\mathbf{H}}(\mathbf{z}) \big|_{\mathbf{y}=\mathbf{0}} = \mathbf{H}(\mathbf{x}) \quad (2.38)$$

in order for the the extended equation to degenerate to the original master equation. Since  $\tilde{\epsilon}(\mathbf{z}) = \tilde{\epsilon}(\mathbf{z} + \mathbf{T}_z)$  where  $T_z$  is any  $n$  dimensional lattice vector, according to the Bloch's theorem we have

$$\tilde{\mathbf{H}}(\mathbf{z}) = \tilde{\mathbf{h}}(\mathbf{z}) e^{i\mathbf{k}_z \cdot \mathbf{z}} \quad (2.39)$$

where  $\tilde{\mathbf{h}}(\mathbf{z})$  possess the same periodicity with  $\tilde{\epsilon}$ , thus both of them can be expanded with respect to the  $n$  dimensional reciprocal lattice vectors

$$\tilde{\mathbf{h}}(\mathbf{z}) = \sum_{\mathbf{G}} \tilde{\mathbf{h}}_{\mathbf{G}} e^{i\mathbf{G}\cdot\mathbf{z}} \quad (2.40)$$

so we have further on

$$\tilde{\mathbf{H}}(\mathbf{z}) = \sum_{\mathbf{G}} \tilde{\mathbf{h}}_{\mathbf{G}} e^{i(\mathbf{k}_z + \mathbf{G})\cdot\mathbf{z}} \quad (2.41)$$

Letting  $\lambda(\mathbf{z}) = \frac{1}{\tilde{\epsilon}(\mathbf{z})}$  with

$$\frac{1}{\tilde{\epsilon}(\mathbf{z})} = \lambda(\mathbf{z}) = \sum_{\mathbf{G}'} \lambda_{\mathbf{G}'} e^{i\mathbf{G}'\cdot\mathbf{z}} \quad (2.42)$$

inserting (2.42) and (2.43) into the modified master equation in supersapce (2.43):

$$\nabla \times \left( \frac{1}{\tilde{\epsilon}(\mathbf{z})} \nabla \times \tilde{\mathbf{H}}(\mathbf{z}) \right) = \left( \frac{\omega}{c} \right)^2 \tilde{\mathbf{H}}(\mathbf{z}) \quad (2.43)$$

we will get

$$\sum_{\mathbf{G}'} \sum_{\mathbf{G}} \nabla \times (\lambda_{\mathbf{G}'} e^{i\mathbf{G}'\cdot\mathbf{z}} \nabla \times (\tilde{\mathbf{h}}_{\mathbf{G}} e^{i((\mathbf{k} + \mathbf{G})\cdot\mathbf{z})})) = \frac{\omega^2}{c^2} \sum_{\mathbf{G}} \tilde{\mathbf{h}}_{\mathbf{G}} e^{i(\mathbf{k}_z + \mathbf{G})\cdot\mathbf{z}} \quad (2.44)$$

which finally results in the set of equations

$$\sum_{\mathbf{G}'} \lambda_{\mathbf{G}-\mathbf{G}'} (\mathbf{k}_x + \mathbf{G}_x) \cdot (\mathbf{k}_x + \mathbf{G}'_x) \tilde{\mathbf{h}}_{\mathbf{G}'} = \left( \frac{\omega^2}{c^2} \right) \tilde{\mathbf{h}}_{\mathbf{G}} \quad (2.45)$$

in which the  $\mathbf{x}$  subscript means taking the physical space projection. During the deduction the relation

$$\mathbf{h} \cdot (\mathbf{k} + \mathbf{G}) = 0 \quad (2.46)$$

has again been used to simplify the equation. Equation (2.45) is the eigenvalue equation for the three dimensional photonic quasicrystal, which is very similiar to the one for conventional periodic dielectric material.



## 2.5 Eigenvalue equation for 1-dimensional quasicrystal

For 1 dimensional quasicrystal (which is physically still 3 dimensional material), the total dimension  $n$  of the superspace is 4, but the permittivity only has 1-dimensional dependence:

$$\epsilon = \epsilon(x_1) \quad (2.47)$$

Similiarly we have the extended permittivity and magnetic field strength:

$$\tilde{\epsilon}(\mathbf{z}) |_{\mathbf{y}=\mathbf{0}} = \epsilon(x_1) \quad (2.48)$$

$$\tilde{\mathbf{H}}(\mathbf{z}) |_{\mathbf{y}=\mathbf{0}} = \mathbf{H}(\mathbf{x}) \quad (2.49)$$

Where  $\tilde{\epsilon}$  is two dimensional periodic in the superspace, which depends on  $z_1$  and  $z_2$ . Therefore it can be written as  $\tilde{\epsilon}(\mathbf{z}')$ , where  $\mathbf{z}'$  has two components  $z_1$  and  $z_2$ , both of which is linear combinations of  $x_1$  and  $y$ . The master equation now reads:

$$\nabla \times \left( \frac{1}{\tilde{\epsilon}(\mathbf{z}')} \nabla \times \tilde{\mathbf{H}}(\mathbf{z}) \right) = \left( \frac{\omega}{c} \right)^2 \tilde{\mathbf{H}}(\mathbf{z}) \quad (2.50)$$

According to the Bloch's theorem, the magnetic field strength in the total space can be written as

$$\tilde{\mathbf{H}}(\mathbf{z}) = \tilde{\mathbf{H}}(\rho, \mathbf{z}') = e^{i\mathbf{k}_{\parallel} \cdot \rho} e^{i\mathbf{k}_{\mathbf{z}'} \cdot \mathbf{z}'} \tilde{\mathbf{h}}(\mathbf{z}') \quad (2.51)$$

where  $\tilde{\mathbf{h}}(\mathbf{z}')$  has  $\mathbf{z}'$  lattice vector periodicity, therefore

$$\tilde{\mathbf{h}}(\mathbf{z}') = \sum_{\mathbf{G}'} \tilde{\mathbf{h}}_{\mathbf{G}'} e^{i\mathbf{G}' \cdot \mathbf{z}'} \quad (2.52)$$

thus

$$\tilde{\mathbf{H}}(\mathbf{z}) = e^{i\mathbf{k}_{\parallel} \cdot \rho} \sum_{\mathbf{G}'} \tilde{\mathbf{h}}_{\mathbf{G}'} e^{i(\mathbf{k}_{\mathbf{z}'} + \mathbf{G}') \cdot \mathbf{z}'} \quad (2.53)$$

$\mathbf{k}_{\parallel}$  denotes the projection of  $\mathbf{k}$  onto the  $\rho$  plane, which is the plane determined by  $x_2$  and  $x_3$ . Assuming  $\tilde{\epsilon}$  being periodic with respect to the lattice vectors of  $z'$  space(2D), we have

$$\frac{1}{\tilde{\epsilon}(\mathbf{z}')} = \lambda(\mathbf{z}') = \sum_{\mathbf{G}''} \lambda_{\mathbf{G}''} e^{i\mathbf{G}'' \cdot \mathbf{z}'} \quad (2.54)$$

We have

$$\begin{aligned}
\nabla \times \tilde{\mathbf{H}}(\mathbf{z}) &= \sum_{\mathbf{G}'} \nabla \times (\tilde{\mathbf{h}}_{\mathbf{G}'} e^{i[\mathbf{k}_{\parallel} \cdot \rho + (\mathbf{k}_{\mathbf{z}'} + \mathbf{G}') \cdot \mathbf{z}']}) \\
&= \sum_{\mathbf{G}'} \nabla \times (\tilde{\mathbf{h}}_{\mathbf{G}'} e^{i[\mathbf{k}_{\parallel} \cdot \mathbf{x} + (\mathbf{k}_{\mathbf{z}'} + \mathbf{G}')_{x_1} \cdot \mathbf{x} + (\mathbf{k}_{\mathbf{z}'} + \mathbf{G}')_y \cdot \mathbf{y}]} ) \\
&= \sum_{\mathbf{G}'} i[\mathbf{k}_{\parallel} + (\mathbf{G}' + \mathbf{k}_{\mathbf{z}'})] e^{i[\mathbf{k}_{\parallel} \cdot \mathbf{x} + (\mathbf{k}_{\mathbf{z}'} + \mathbf{G}')_{x_1} \cdot \mathbf{x} + (\mathbf{k}_{\mathbf{z}'} + \mathbf{G}')_y \cdot \mathbf{y}]} \times \tilde{\mathbf{h}}_{\mathbf{G}'}
\end{aligned} \tag{2.55}$$

$$\begin{aligned}
&\nabla \times \left( \frac{1}{\tilde{\epsilon}(\mathbf{z}')} \nabla \times \tilde{\mathbf{H}}(\mathbf{z}) \right) \\
&= i \nabla \times \sum_{\mathbf{G}''} \sum_{\mathbf{G}'} \lambda_{\mathbf{G}''} e^{i\mathbf{G}'' \cdot \mathbf{z}'} e^{i[\mathbf{k}_{\parallel} \cdot \mathbf{x} + (\mathbf{k}_{\mathbf{z}'} + \mathbf{G}')_{x_1} \cdot \mathbf{x} + (\mathbf{k}_{\mathbf{z}'} + \mathbf{G}')_y \cdot \mathbf{y}]} \\
&\quad \cdot [\mathbf{k}_{\parallel} + (\mathbf{G}' + \mathbf{k}_{\mathbf{z}'})] \times \tilde{\mathbf{h}}_{\mathbf{G}'} \\
&= -i^2 \sum_{\mathbf{G}''} \sum_{\mathbf{G}'} \lambda_{(\mathbf{G}''' - \mathbf{G}')} e^{i[\mathbf{k}_{\parallel} \cdot \rho + (\mathbf{G}''' + \mathbf{k}_{\mathbf{z}'}) \cdot \mathbf{z}']} \{ [\mathbf{k}_{\parallel} + (\mathbf{G}' + \mathbf{k}_{\mathbf{z}'})_{x_1}] \times \tilde{\mathbf{h}}_{\mathbf{G}'} \} \\
&\quad \times [\mathbf{k}_{\parallel} + (\mathbf{G}''' + \mathbf{k}_{\mathbf{z}'})_{x_1}] \\
&= \sum_{\mathbf{G}'''} \sum_{\mathbf{G}'} \lambda_{(\mathbf{G}''' - \mathbf{G}')} e^{i[\mathbf{k}_{\parallel} \cdot \rho + (\mathbf{G}''' + \mathbf{k}_{\mathbf{z}'}) \cdot \mathbf{z}']} [\mathbf{k}_{\parallel} + (\mathbf{G}' + \mathbf{k}_{\mathbf{z}'})_{x_1}] \cdot [\mathbf{k}_{\parallel} + (\mathbf{G}''' + \mathbf{k}_{\mathbf{z}'})_{x_1}] \tilde{\mathbf{h}}_{\mathbf{G}'} \\
&= \frac{\omega^2}{c^2} \sum_{\mathbf{G}'''} e^{i[\mathbf{k}_{\parallel} \cdot \rho + (\mathbf{G}''' + \mathbf{k}_{\mathbf{z}'}) \cdot \mathbf{z}']} \tilde{\mathbf{h}}_{\mathbf{G}'''}
\end{aligned} \tag{2.56}$$

where  $\mathbf{G}''' := \mathbf{G}' + \mathbf{G}''$ . Thus we have

$$\sum_{\mathbf{G}'} \lambda_{(\mathbf{G}''' - \mathbf{G}')} [\mathbf{k}_{\parallel} + (\mathbf{G}' + \mathbf{k}_{\mathbf{z}'})_{x_1}] \cdot [\mathbf{k}_{\parallel} + (\mathbf{G}''' + \mathbf{k}_{\mathbf{z}'})_{x_1}] \tilde{\mathbf{h}}_{\mathbf{G}'} = \frac{\omega^2}{c^2} \tilde{\mathbf{h}}_{\mathbf{G}'''} \tag{2.57}$$

in equivalence this equation can be written as

$$\sum_{\mathbf{G}'} \lambda_{(\mathbf{G} - \mathbf{G}')} [\mathbf{k}_{\parallel} + (\mathbf{G}' + \mathbf{k}_{\mathbf{z}'})_{x_1}] \cdot [\mathbf{k}_{\parallel} + (\mathbf{G} + \mathbf{k}_{\mathbf{z}'})_{x_1}] \tilde{\mathbf{h}}_{\mathbf{G}'} = \frac{\omega^2}{c^2} \tilde{\mathbf{h}}_{\mathbf{G}} \tag{2.58}$$

which can be further simplified as:

$$\sum_{\mathbf{G}'} \lambda_{(\mathbf{G} - \mathbf{G}')} [\mathbf{k}_{\parallel}^2 + (\mathbf{G}' + \mathbf{k}_{\mathbf{z}'})_{x_1} \cdot (\mathbf{G} + \mathbf{k}_{\mathbf{z}'})_{x_1}] \tilde{\mathbf{h}}_{\mathbf{G}'} = \frac{\omega^2}{c^2} \tilde{\mathbf{h}}_{\mathbf{G}} \tag{2.59}$$

because of the fact that  $\mathbf{k}_{\parallel}$  is perpendicular to the  $x_1$  direction. For the ideal case, the quasicrystal as well as the corresponding periodic superlattice is unbounded, thus

$\mathbf{k}_{\parallel}$  can be set to zero because of the full symmetry in the plane perpendicular to  $x_1$  direction. Therefore, the equation we will use to calculate the photonic band structure is:

$$\sum_{\mathbf{G}'} \lambda_{(\mathbf{G}-\mathbf{G}')} (\mathbf{G}' + \mathbf{k})_{x_1} \cdot (\mathbf{G} + \mathbf{k})_{x_1} \tilde{\mathbf{h}}_{\mathbf{G}'} = \frac{\omega^2}{c^2} \tilde{\mathbf{h}}_{\mathbf{G}} \quad (2.60)$$

which is similar to the one for one dimensional periodic crystal, but the  $\mathbf{G}$ s are two dimensional reciprocal lattice vectors, which has to be projected on the direction of the one dimensional quasicrystal chain.

By solving the eigenvalue matrix equation (2.45) eigenvalues can be obtained, which is used to construct the photonic bandstructure. We can not obtain full knowledge about the extended magnetic field strength  $\tilde{\mathbf{H}}$ .  $\tilde{\mathbf{H}}$  is just demanded to degenerate to physical magnetic field strength  $\mathbf{H}$  when  $\mathbf{y}$  is an arbitrary constant. The reason why the constant is arbitrary is because the cut plane is irrational, which will pass through every point of the unit cell of the superspace.

## Chapter 3

# Method for numerical calculation of the band structure of a one dimensional photonic quasicrystal

Considering the one dimensional Fibonacci-like quasicrystal. In principle the eigenvalue equation is actually an infinite dimensional matrix for the number of all the reciprocal lattice vectors  $\mathbf{G}$  is infinite. But in order to obtain the eigenvalues of it numerically, only finite number of reciprocal lattice vectors should be considered, which can be chosen differently.

It should be reasonably conjectured that as more reciprocal vectors are chosen, the resulting photonic band structure is approaching the one for the infinite matrix, since the original eigenvalue matrix equation includes all the  $\mathbf{G}s$ .

We now write the eigenvalue equation in the form of matrix equation

$$\mathbf{M}\beta = \frac{\omega^2}{c^2}\beta \quad (3.1)$$

where  $\mathbf{M}$  is a matrix of which the  $\mathbf{G}\mathbf{G}'$  element is  $\lambda_{\mathbf{G}-\mathbf{G}'}(\mathbf{G}' + \mathbf{k}_x)(\mathbf{G} + \mathbf{k}_x)$  and  $\beta$  is the vector composed of all the fourier coefficients  $\tilde{\mathbf{h}}_{\mathbf{G}s}$ . Each matrix element of  $\mathbf{M}$  has to be given in order to carry out the computation, for the sake of which the reciprocal lattice vectors has to be numbered by natural numbers for conveniency. Thus supposing the set of  $\mathbf{G}s$  are chosen to be all the reciprocal lattice vectors inside the box shown in Figure 3.1, of which the center is the origin of reciprocal space. Any

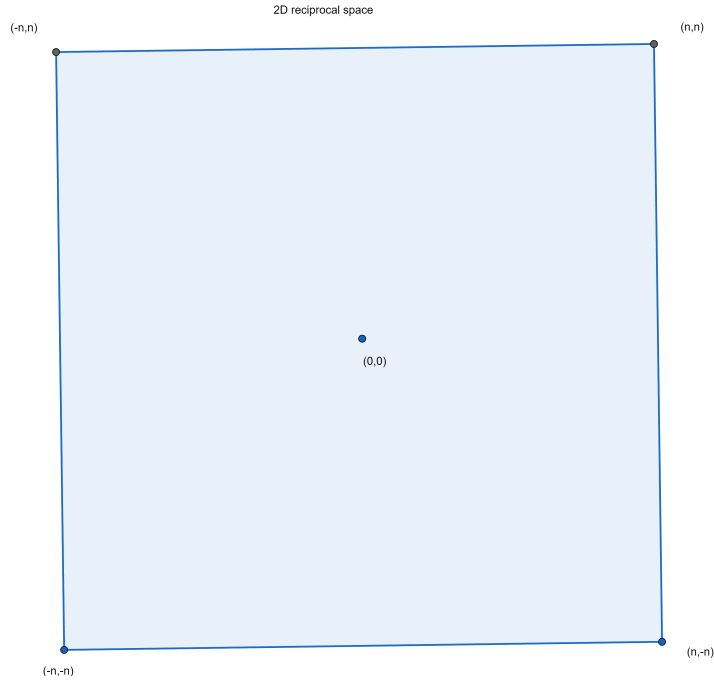


FIGURE 3.1: A square area around the origin of the reciprocal space from inside of which all the  $\mathbf{G}$ s are used in the calculation

reciprocal lattice vectors for two dimensional periodic square lattice  $\mathbf{G}$  can be written as:

$$\mathbf{G} = 2\pi\left(\frac{m_1}{a}\hat{\mathbf{a}}_1 + \frac{m_2}{a}\hat{\mathbf{a}}_2\right) \quad (3.2)$$

where  $a$  is the lattice constant of the 2D square lattice, of which  $\hat{\mathbf{a}}_1$  and  $\hat{\mathbf{a}}_2$  are the unit basis. For conveniency we can set  $a$  to be 1. For the choice of  $\mathbf{G}$ s mentioned above there are clearly  $(2n + 1)^2$  reciprocal lattice vectors in the box, each of which can be numbered with the following functions:

$$\mathbf{G}_i = 2\pi(m_1(i)\hat{\mathbf{a}}_1 + m_2(i)\hat{\mathbf{a}}_2) \quad (3.3)$$

in which

$$m_1(i) = -n + \lfloor \frac{i-1}{2n+1} \rfloor \quad (3.4)$$

and

$$m_2(i) = -n - 1 + i - \lfloor (2n+1)\frac{i-1}{2n+1} \rfloor \quad (3.5)$$

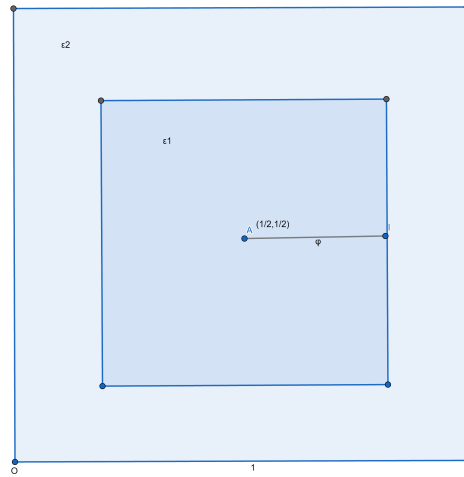


FIGURE 3.2: Unit cell of the two dimensional super space from which one dimensional quasicrystal is generated

where  $[x]$  is the floor function which gives the largest integer not larger than  $x$ . The numbering works in the following way:

$$\begin{aligned}
 1 &: (-n, -n) \\
 2 &: (-n, -n + 1) \\
 &\dots\dots\dots \\
 2n + 1 &: (-n, n) \\
 2n + 2 &: (-n + 1, -n) \\
 &\dots\dots\dots \\
 (2n + 1)^2 &: (n, n)
 \end{aligned} \tag{3.6}$$

therefore each matrix element of  $\mathbf{M}_{ij}$  is determined. As long as the permittivity distribution  $\epsilon$  is given, the eigenvalues of the matrix can be calculated by solving the eigenvalue matrix equation.

During the study it was found that the calculation of fourier coefficients  $\lambda_{\mathbf{G}}$  will cost most time if the integral computation were done numerically. So if it is possible to find permittivity distribution for which the  $\lambda_{\mathbf{G}}$  can be theoretical greatly simplified, the computation running time will greatly decrease. Figure 3.2 shows a unit cell in the superspace(ignoring the two irrelevant directions). In each unit cell there is a

square area of embedded dielectric material with different permittivity from its adjacent dielectric material.

Point  $A$  is the center of both squares in the graph, of which the coordinates are  $(\frac{1}{2}, \frac{1}{2})$ . The two dimensional fourier coefficients can be calculated through the following integral:

$$\lambda_{\mathbf{G}'} = \int_V \lambda(\mathbf{z}) e^{-i\mathbf{G}' \cdot \mathbf{z}} d\mathbf{z} \quad (3.7)$$

on account of the fact that

$$\lambda(\mathbf{z}) = \sum_{\mathbf{G}} \lambda_{\mathbf{G}} e^{i\mathbf{G} \cdot \mathbf{z}} \quad (3.8)$$

according to the Bloch theorem, where  $V$  is the volume of the unit cell, which is 1 if the lattice constant is 1. The distribution of the reciprocal of permittivity is described generally as:

$$\lambda(\mathbf{z}) = \begin{cases} \alpha, & \frac{1}{2} - \varphi \leq z_1, z_2 \leq \frac{1}{2} + \varphi \\ \beta, & \text{else where in the unit cell} \end{cases} \quad (3.9)$$

where  $\varphi$  is half the side length of the smaller square. Therefore:

$$\lambda_{\mathbf{G}} = \int_1 \alpha e^{-i\mathbf{G} \cdot \mathbf{z}} d\mathbf{z} + \int_2 \beta e^{-i\mathbf{G} \cdot \mathbf{z}} d\mathbf{z} \quad (3.10)$$

where the subscripts 1 and 2 refer to two areas of the unit cell with different permittivities. Further on we have:

$$\begin{aligned} \lambda_{\mathbf{G}} &= \int_1 \alpha e^{-i\mathbf{G} \cdot \mathbf{z}} d\mathbf{z} + \int_{1 \text{ and } 2} \beta e^{-i\mathbf{G} \cdot \mathbf{z}} d\mathbf{z} - \int_1 \beta e^{-i\mathbf{G} \cdot \mathbf{z}} d\mathbf{z} \\ &= \int_1 (\alpha - \beta) e^{-i\mathbf{G} \cdot \mathbf{z}} d\mathbf{z} + \int_{1 \text{ and } 2} \beta e^{-i\mathbf{G} \cdot \mathbf{z}} d\mathbf{z} \end{aligned} \quad (3.11)$$

for clearness the two terms in equation (3.11) are calculated distinctly.

$$\int_1 (\alpha - \beta) e^{-i\mathbf{G} \cdot \mathbf{z}} d\mathbf{z} = (\alpha - \beta) \int_{\frac{1}{2}-\varphi}^{\frac{1}{2}+\varphi} e^{-iG_1 z_1} dz_1 \int_{\frac{1}{2}-\varphi}^{\frac{1}{2}+\varphi} e^{-iG_2 z_2} dz_2 \quad (3.12)$$

in which :

$$\int_{\frac{1}{2}-\varphi}^{\frac{1}{2}+\varphi} e^{-iG_1 z_1} dz_1 = 2\varphi \text{ if } G_1 = 0 \quad (3.13)$$

for the case when  $G_1 \neq 0$

$$\begin{aligned} \int_{\frac{1}{2}-\varphi}^{\frac{1}{2}+\varphi} e^{-iG_1 z_1} dz_1 &= \frac{i}{G_1} (e^{-iG_1(\frac{1}{2}+\varphi)} - e^{-iG_1(\frac{1}{2}-\varphi)}) \\ &= \frac{2}{G_1} \sin(G_1\varphi) e^{-\frac{i}{2}G_1} \end{aligned} \quad (3.14)$$

thus we have

$$\int_1 (\alpha - \beta) e^{-i\mathbf{G} \cdot \mathbf{z}} d\mathbf{z} = \begin{cases} 4(\alpha - \beta)\varphi^2, & G_1 = 0, G_2 = 0 \\ \frac{4(\alpha - \beta)}{G_1 G_2} \sin(G_1\varphi) \sin(G_2\varphi) e^{-\frac{i}{2}(G_1 + G_2)}, & G_1 \neq 0, G_2 \neq 0 \\ \frac{4\varphi(\alpha - \beta)}{G_1} \sin(G_1\varphi) e^{-\frac{i}{2}G_1}, & G_1 \neq 0, G_2 = 0 \\ \frac{4\varphi(\alpha - \beta)}{G_2} \sin(G_2\varphi) e^{-\frac{i}{2}G_2}, & G_1 = 0, G_2 \neq 0 \end{cases} \quad (3.15)$$

similarly, for the integral in the whole unit cell (area 1 and 2) we have

$$\int_{1 \text{ and } 2} \beta e^{-i\mathbf{G} \cdot \mathbf{z}} d\mathbf{z} = \begin{cases} \beta, & G_1 = 0, G_2 = 0 \\ \frac{4\beta}{G_1 G_2} \sin \frac{G_1}{2} \sin \frac{G_2}{2} e^{-\frac{i}{2}(G_1 + G_2)}, & G_1 \neq 0, G_2 \neq 0 \\ \frac{2\beta}{G_1} \sin \frac{G_1}{2} e^{-\frac{i}{2}G_1}, & G_1 \neq 0, G_2 = 0 \\ \frac{2\beta}{G_2} \sin \frac{G_2}{2} e^{-\frac{i}{2}G_2}, & G_1 = 0, G_2 \neq 0 \end{cases} \quad (3.16)$$

where the components  $G_1$  and  $G_2$  can certainly be written as

$$G_1 = 2\pi m_1, G_2 = 2\pi m_2 \quad (3.17)$$

according to equation (3.3). With this in mind, the relation (3.16) can be greatly simplified because each term including  $\sin \frac{G_1}{2}$  or  $\sin \frac{G_2}{2}$  is zero. So the final result of the integral is:

$$\lambda_{\mathbf{G}} = \begin{cases} 4(\alpha - \beta)\varphi^2 + \beta, & G_1 = 0, G_2 = 0 \\ \frac{4(\alpha - \beta)}{G_1 G_2} \sin(G_1\varphi) \sin(G_2\varphi) e^{-\frac{i}{2}(G_1 + G_2)}, & G_1 \neq 0, G_2 \neq 0 \\ \frac{4\varphi(\alpha - \beta)}{G_1} \sin(G_1\varphi) e^{-\frac{i}{2}G_1}, & G_1 \neq 0, G_2 = 0 \\ \frac{4\varphi(\alpha - \beta)}{G_2} \sin(G_2\varphi) e^{-\frac{i}{2}G_2}, & G_1 = 0, G_2 \neq 0 \end{cases} \quad (3.18)$$

Now that the fourier coefficient of  $\lambda$  for each  $\mathbf{G}$  is analytically represented, it will be ready to put them into the matrix to get the elements without calculating the integral numerically, making the computation much faster.



Since the choice of reciprocal lattice vectors is not unique, the corresponding photonic bandstructures calculated may not be identical for different sets of  $\mathbf{G}s$ , the results of which are shown in the next chapter.

## Chapter 4

# Results and discussion

In the following sections band structures are calculated for two dimensional square photonic crystals and one dimensional Fibonacci-like quasicrystals.

### 4.1 Band structures of two dimensional square photonic crystals

In order to test the methods used to calculate the photonic bands structure, the more common photonic crystals instead of quasicrystals are considered in the first place. For the sake of consistency we consider the two dimensional square lattice described in Figure 4.1 , similar to the periodic square lattice in the superspace for the one dimensional quasicrystal case.

In the unit cell of the lattice certain dielectric material is embedded, while the complementary region of the unit cell is filled with material whose permittivity is different from inside the embedded region. The permittivities of the two regions are

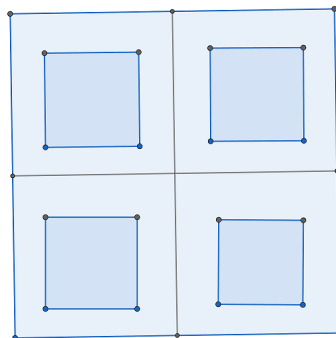


FIGURE 4.1: Two dimensional square lattice photonic crystal. There are two regions inside one unit cell of which the permittivity is different.

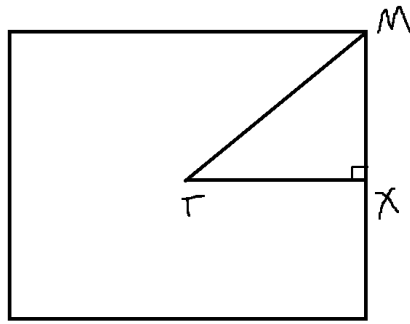
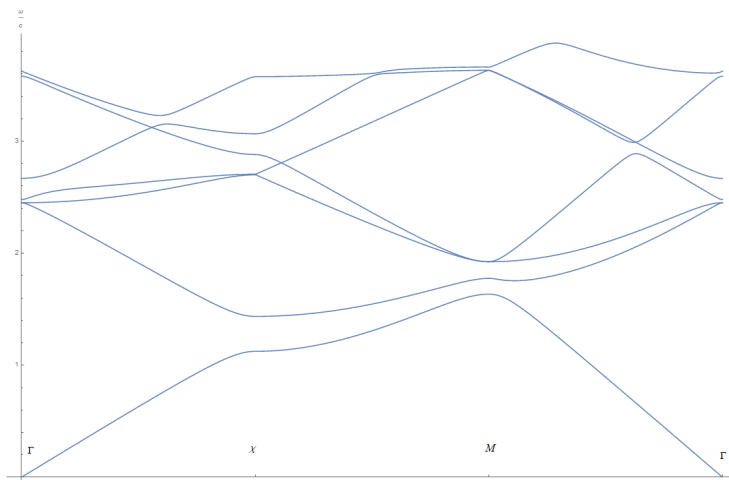


FIGURE 4.2

FIGURE 4.3: Band structure for two dimensional square-like photonic crystal with  $\omega_1 : \omega_2 = 1 : 3$ .

named  $\omega_1$  for inside the embedding and  $\omega_2$  for the rest of the cell respectively. The reciprocal lattices vectors chosen for the computation are those  $\mathbf{G}$ s around the origin of the reciprocal space and fulfilling the requirements that:

$$-3 \cdot 2\pi \leq G_1, G_2 \leq 3 \cdot 2\pi \quad (4.1)$$

where  $G_1$  and  $G_2$  are two components of  $\mathbf{G}$  with respect to the two perpendicular axis.

In the Figures 4.3~4.6 for two dimensional photonic crystal with the specified geometry structure described above and with different ratio of permittivity photonic bandstructures are obtained. Figure shows the first Brillouin zone of the square lattice and three representative points in it are denote as  $\Gamma, \chi$  and  $M$ .

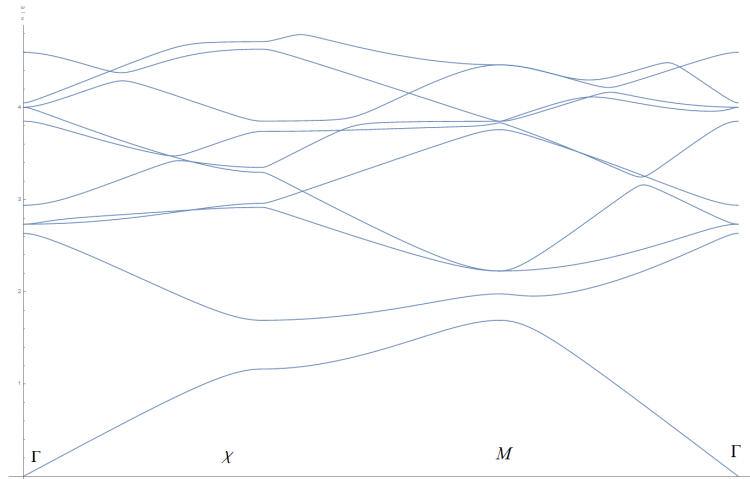


FIGURE 4.4: Band structure for two dimensional square-like photonic crystal with  $\omega_1 : \omega_2 = 1 : 5$ .

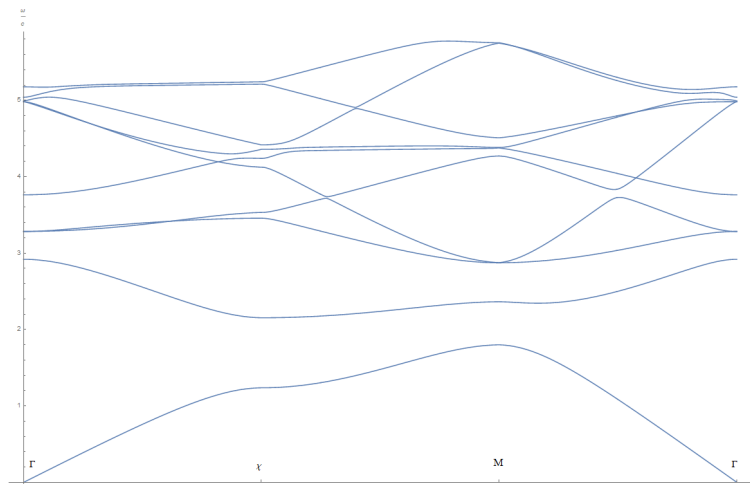


FIGURE 4.5: Band structure for two dimensional square-like photonic crystal with  $\omega_1 : \omega_2 = 1 : 10$

For permittivity ratio  $\omega_1 : \omega_2 = 1 : 3$ , the photonic bandstructure is shown in Figure 4.3, where we can see that there isn't any band gaps appearing.

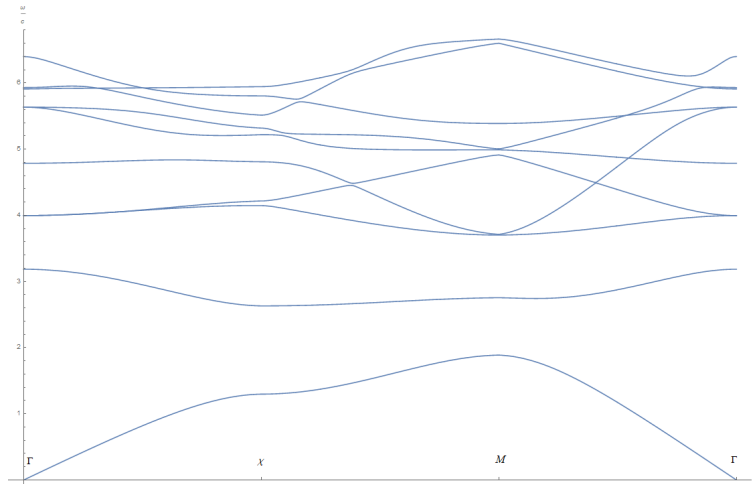


FIGURE 4.6: Band structure for two dimensional square-like photonic crystal with  $\omega_1 : \omega_2 = 20 : 1$

While when the ratio of permittivity increases, the bands bend inwards (Figure 4.4), and when the ratio gets large enough there appears a band gap in the lower part of the band structure between the first band and the second band, as shown in Figure 4.5. And when the ratio of permittivity increases further, the band gap becomes wider, which is demonstrated in Figure 4.6. Meanwhile, a new band gap arises between the second band and the third band. Then we increase the number of reciprocal lattice vectors to calculate the band structure and compare it with the one for fewer  $\mathbf{G}s$ , it is found that the calculated band structure are almost the same, as shown in Figure 4.7 and Figure 4.8.

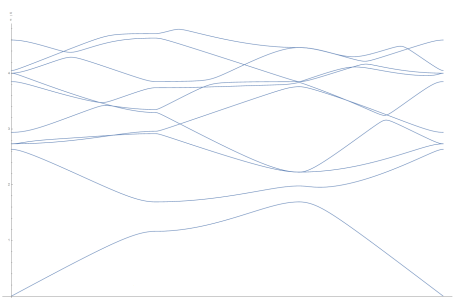


FIGURE 4.7: Photonic bandstructure calculated using 49 reciprocal lattice vectors

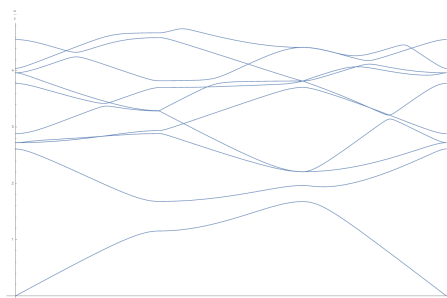


FIGURE 4.8: Photonic bandstructure calculated using 289 reciprocal lattice vectors

Figure 4.9 is the band structure of a square photonic crystal with square dielectric rods in air, the form of which is in agreement with the result obtained in this thesis.

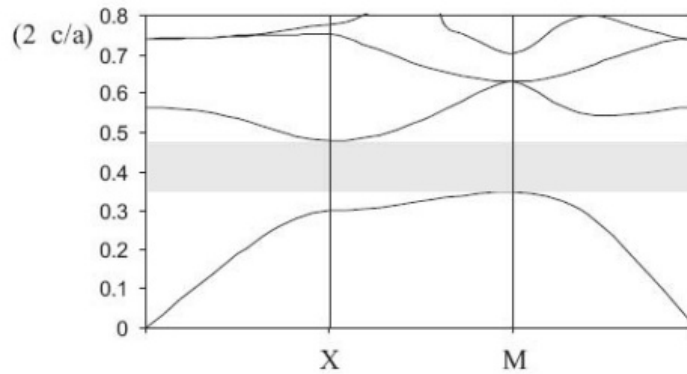


FIGURE 4.9: The band-gap structure of the photonic crystal consisting of a square lattice of square dielectric rods ( $n=3.4$ ) in an air background. The ratio of the side of the rods to the crystal period is  $d/a=0.25$ .

## 4.2 Band structures of one dimensional Fibonacci-like photonic quasicrystals

As discussed before, the geometry structure of the quasiperiodic material that will be studied is the one dimensional Fibonacci like quasicrystal generated by irrational cutting from two dimensional periodic square lattice. This so called Fibonacci-like chain is not exactly the original Fibonacci chain, which can certainly also be generated through the same method, while the sides of the embedding square will not be parallel to the sides of the square unit cell but has an intersection angle inbetween, as shown in Figure 4.10, where the unit cell is the square constructed by connecting center of four blue squares, while AB is the irrational cut line(plane). For the sake of computation efficiency, the former one will be studied. Throughout the computation, the half side length of the inner square  $\varphi$ (Figure 3.2) is set to be  $\frac{1}{3}$ , while different permittivity ratios are adopted to calculate corresponding photonic bandstructure. In this part the photonic band structures of one dimensional Fibonacci-like chains with different permittivity ratio are calculated, while different numbers of reciprocal lattice vectors are used as parameters to see how the results will depend on them. Consider the extrem case that  $\omega_1 = \omega_2$  in the first place, which is actually not quasicrystal but uniform unbounded dielectric material, so the magnetic waves in it can only be plane

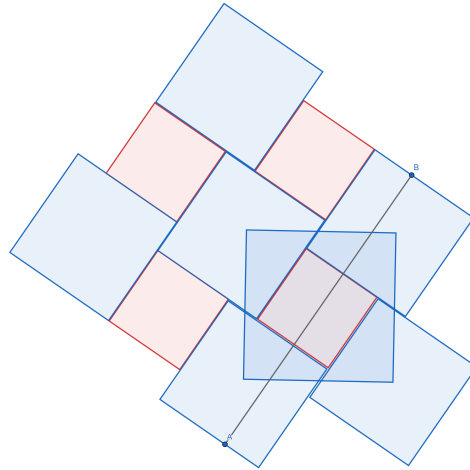


FIGURE 4.10: One dimensional fibonacci chain generated from irrational cut of a two dimensional periodic superspace.

waves. In the uniform material the frequency  $\omega$  is proportional to the wave number  $k$ , thus the bands are merely straight lines.

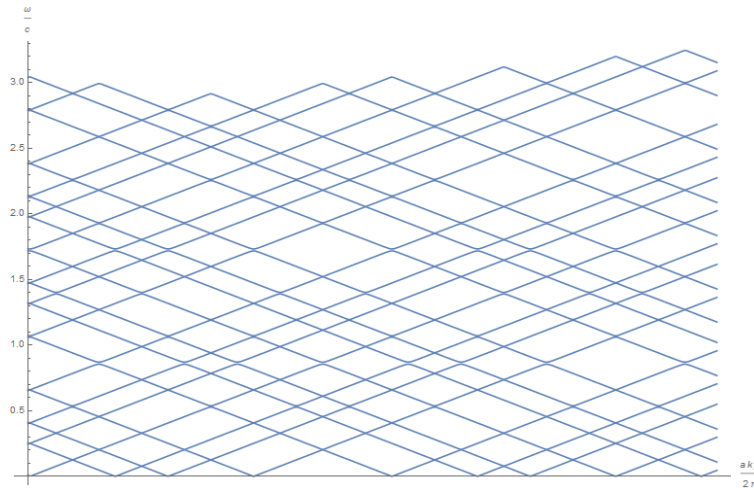


FIGURE 4.11: Band structure for one dimensional Fibonacci-like photonic quasicrystal generated from irrational cutting from two dimensional periodic square lattice. The ratio of permittivities is  $\epsilon_1 : \epsilon_2 = 11 : 10$ . The number of reciprocal lattice vectors used in the calculation is  $11^2 = 121$ , uniformly distributed in a square around the origin of the reciprocal space.

In Figure 4.11 the band structure is very close to a set of plane waves but with small gaps between some curves, for the ratio of permittivity is close to one. When the ratio of permittivity increases, the band structure deviates from plane waves and a photonic band gap can be seen around the position  $\frac{\omega}{c} = 0.9$ , as we can see in Figure 4.12.

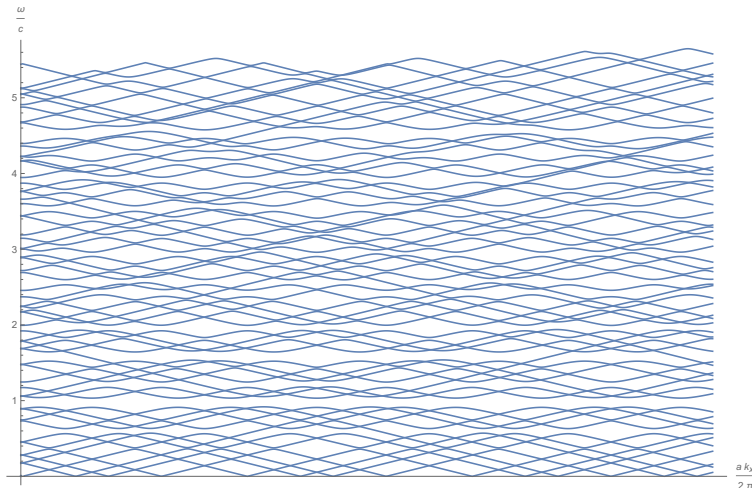


FIGURE 4.12: Band structure for one dimensional Fibonacci-like photonic quasicrystal generated from irrational cutting from two dimensional periodic square lattice. The ratio of permittivities is  $\omega_1 : \omega_2 = 1 : 2$ . Number of reciprocal lattice vectors used: 121

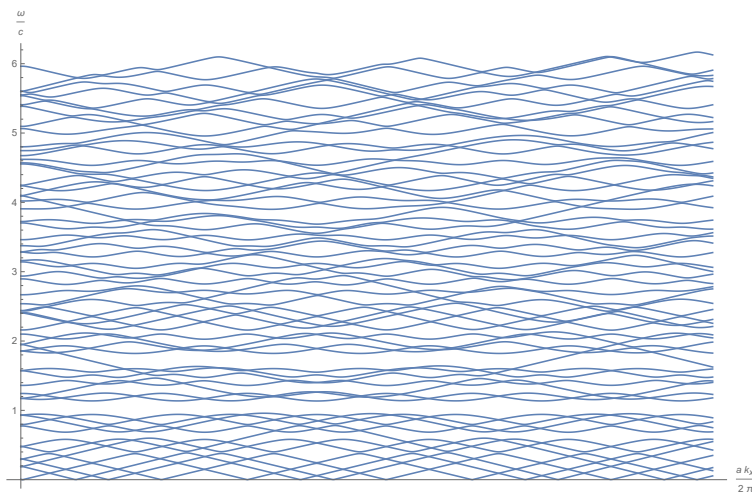


FIGURE 4.13: Band structure for one dimensional Fibonacci-like photonic quasicrystal generated from irrational cutting from two dimensional periodic square lattice. The ratio of permittivities is  $\omega_1 : \omega_2 = 1 : 3$ . Number of reciprocal lattice vectors used: 121

As ratio of permittivities increases further, the band gap remains at the same position, as shown in Figure 4.14, until when the ratio gets too large (e.g. 1:50), in which case the band gap doesn't exist anymore, as shown in Figure 4.15.

Figure 4.18 is the photonic bandstructure for  $\omega_1 : \omega_2 = 1 : 10$  but the number of reciprocal lattice vectors used is increased to  $17^2 = 289$ . Comparing the result with the one having the same permittivity ratio using fewer  $\mathbf{G}$ s, we will found that the bandstructures have similiar distributions but the bands within a given width for the latter is relatively denser. This means that increasing the number of reciprocal



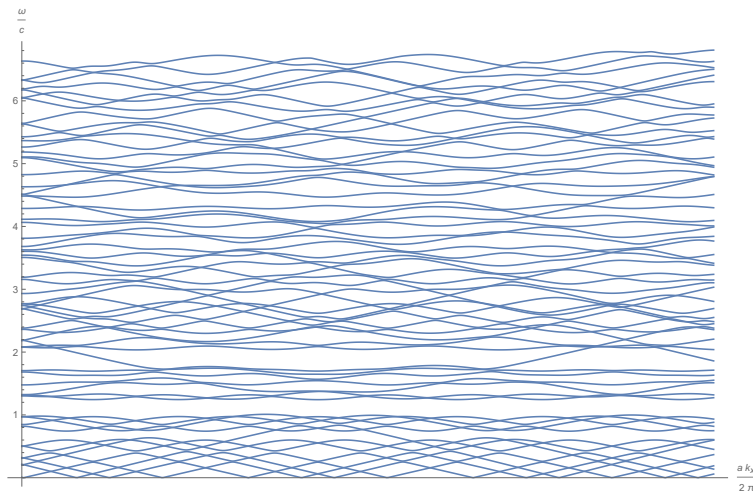


FIGURE 4.14: Band structure for one dimensional Fibonacci-like photonic quasicrystal generated from irrational cutting from two dimensional periodic square lattice. The ratio of permittivities is  $\omega_1 : \omega_2 = 1 : 5$

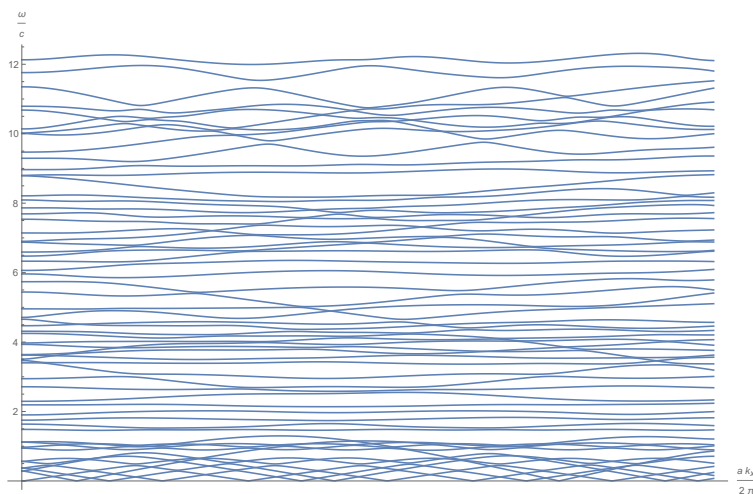


FIGURE 4.15: Band structure for one dimensional Fibonacci-like photonic quasicrystal generated from irrational cutting from two dimensional periodic square lattice. The ratio of permittivities is  $\omega_1 : \omega_2 = 1 : 50$ . Number of reciprocal lattice vectors used: 121

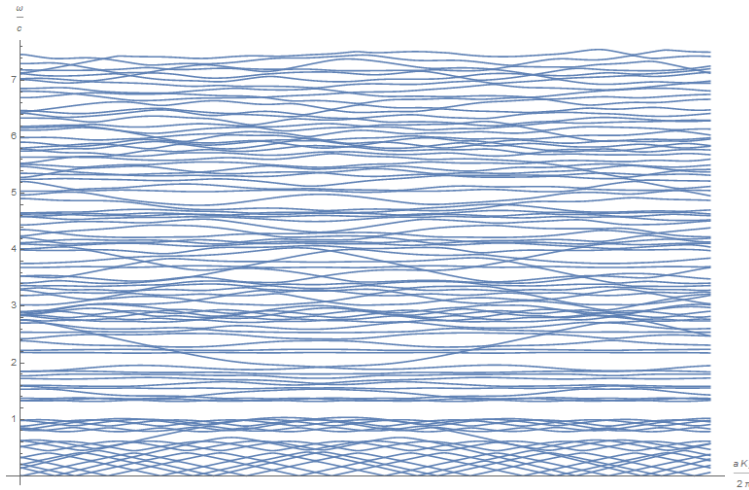


FIGURE 4.16: Band structure for one dimensional Fibonacci-like photonic quasicrystal generated from irrational cutting from two dimensional periodic square lattice. The ratio of permittivities is  $\omega_1 : \omega_2 = 1 : 10$ . Number of reciprocal lattice vectors used: 289

lattice vectors in the calculation results in higher resolution of the bandstructure. It is different from the situation for normal periodic photonic crystal, of which the density of bands won't get larger for increasing number of the set of  $\mathbf{G}s$  chosen. Therefore, increasing number of  $\mathbf{G}s$  won't result in higher resolution, but added more bands above the former band structure, extending the photonic band structure to higher frequency.

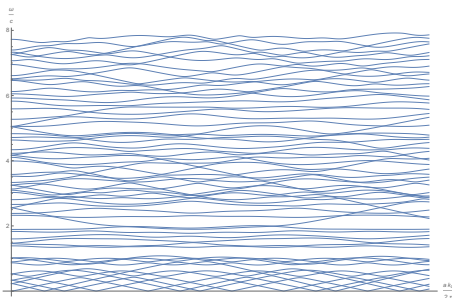


FIGURE 4.17: Band structure calculated for one dimensional Fibonacci-like photonic quasicrystal using 121 reciprocal lattice vectors

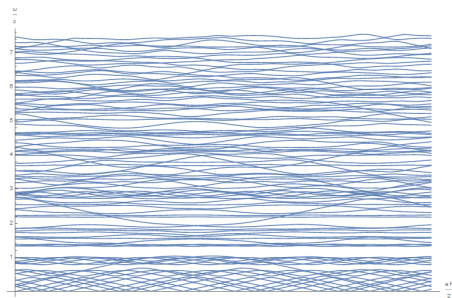


FIGURE 4.18: Band structure calculated for one dimensional Fibonacci-like photonic quasicrystal using 289 reciprocal lattice vectors

Considering translating the reciprocal lattice vectors used in calculation in such a way:

$$\mathbf{G} \rightarrow \mathbf{G} + \mathbf{T} \quad (4.2)$$

As we can see in the matrix equation:

$$\sum_{\mathbf{G}'} \lambda_{\mathbf{G}-\mathbf{G}'} (\mathbf{k} + \mathbf{G}) \cdot (\mathbf{k} + \mathbf{G}') \mathbf{h}_{\mathbf{G}'} = \left(\frac{\omega^2}{c^2}\right) \mathbf{h}_{\mathbf{G}} \quad (4.3)$$

The translation vector  $\mathbf{T}$  can act on  $\mathbf{k}$  instead of  $\mathbf{G}$ , which is equivalent to the former. Therefore the obtained photonic band structure will be the same, only with a translation of the coordinates.

## Chapter 5

# Summary and Outlook

### 5.1 Summary of results

In the theoretical part of this thesis, the Master equation for dielectric material is deduced from Macroscopic Maxwell equations. Then the magnetic field strength  $\mathbf{H}$  are expanded as plane waves according to the Bloch theory, while the periodic permittivity  $\epsilon(\mathbf{r})$  is expanded as fourier series with respect to the reciprocal lattice vectors. By substituting them into the Master equation we obtained a eigenvalue matrix equation from which the photonic band structure of photonic crystal ( $\omega \sim k$ ) can be calculated. For the case of quasicrystal, since it can be seen as cross section of a higher dimensional periodic superspace, the Master equation can be modified to calculate the photonic band structure, taking advantage of the fact that the permittivity being periodic with respect to the superspace, which makes the Bloch theory applicable. In the numerical calculation part, the photonic band structures of both two dimensional periodic square crystal and one dimensional Fibonacci-like quasicrystal are computed for various different ratios of permittivities. By comparing the results we found that for two dimensional square crystals, band gaps won't appear until the ratio of permittivity is large enough ( $\omega_2 : \omega_1 \sim 10$ ), when there is a band gap visible, while the width of the gap will increase and another band gap will arise, as the ratio of permittivity gets larger. For one dimensional quasicrystal, a band gap can almost always been found if the ratio of permittivities are not one, unless when it gets too large (e.g. larger than 50). In the latter case, the band gap disappears and the bands get squeezed together at the position where the band gap exists for lower ratio of permittivity. We have

noticed that by using different numbers of reciprocal lattice vectors in the calculation, the resolution of the band structure is affected, which is positively correlated to the number of  $\mathbf{G}$ s while the structure of the band remains the same, thus the position and width of the band gap is also unchanged.

## 5.2 Outlook

During the computation of this thesis it was found that if the calculation of Fourier coefficients of the reciprocal of permittivity are not done analytically but numerically, much more calculation time will be needed. So for two or three dimensional quasicrystals, since the superspace from which they are generated are of higher dimensions, the increasement of the number of reciprocal lattice vectors as well as the more complex integral may lead to greater computation difficulty. It is suggested that the region of the embedded material in the unit cell of the superlattice being chosen such that the corresponding fourier coefficients are elementary functions, which will greatly simplify the calculation.

# Bibliography

- De Bruijn, N G (1981). “Algebraic theory of Penrose’s non-periodic tilings of the plane. I, II : dedicated to G. Pólya”. In: *Pólya. Indagationes Mathematicae* 43.1, pp. 39–66. URL: <https://pure.tue.nl/ws/files/4344195/597566.pdf>.
- Duneau, Michel and André Katz (1985). “Quasiperiodic Patterns”. In: *Physical Review Letters* 54.25, pp. 2688–2691. ISSN: 0031-9007. DOI: [10.1103/PhysRevLett.54.2688](https://doi.org/10.1103/PhysRevLett.54.2688). URL: <https://link.aps.org/doi/10.1103/PhysRevLett.54.2688>.
- Elser, Veit (1985). “Indexing problems in quasicrystal diffraction”. In: *Physical Review B* 32.8, pp. 4892–4898. ISSN: 0163-1829. DOI: [10.1103/PhysRevB.32.4892](https://doi.org/10.1103/PhysRevB.32.4892). URL: <https://link.aps.org/doi/10.1103/PhysRevB.32.4892>.
- Gahler, F and J Rhyner (1986). “Equivalence of the generalised grid and projection methods for the construction of quasiperiodic tilings”. In: *J. Phys. A: Math. Gen.* *J. Phys. A: Math. Gen* 19.19, pp. 267–277. URL: <http://iopscience.iop.org/article/10.1088/0305-4470/19/2/020/pdf>.
- Hwang, Dae-Kue, Byunghong Lee, and Dae-Hwan Kim (2013). “Efficiency enhancement in solid dye-sensitized solar cell by three-dimensional photonic crystal”. In: *RSC Advances* 3.9, p. 3017. ISSN: 2046-2069. DOI: [10.1039/c2ra22746k](https://doi.org/10.1039/c2ra22746k). URL: <http://xlink.rsc.org/?DOI=c2ra22746k>.
- Jackson, John David (1999). *Classical electrodynamics*. Wiley, p. 808. ISBN: 9780471309321.
- Joannopoulos, J. D. (John D.) (2008). *Photonic crystals : molding the flow of light*. Princeton University Press, p. 286. ISBN: 9780691124568. URL: <https://press.princeton.edu/titles/8696.html>.
- Knittl, Zdenek. (1976). *Optics of thin films; an optical multilayer theory*. Wiley, p. 548. ISBN: 047149531X. URL: [https://books.google.de/books/about/Optics\\_of\\_Thin\\_Films.html?id=vCu9AQAACAAJ&redir\\_esc=y](https://books.google.de/books/about/Optics_of_Thin_Films.html?id=vCu9AQAACAAJ&redir_esc=y).
- Kramer, P., R. Neri, and IUCr (1984). “On periodic and non-periodic space fillings of  $E^m$  obtained by projection”. In: *Acta Crystallographica Section A Foundations of*

- Crystallography* 40.5, pp. 580–587. ISSN: 0108-7673. DOI: [10.1107/S0108767384001203](https://doi.org/10.1107/S0108767384001203).  
URL: <http://scripts.iucr.org/cgi-bin/paper?S0108767384001203>.
- Kraus, Yaacov E. and Oded Zilberberg (2016). “Quasiperiodicity and topology transcend dimensions”. In: *Nature Physics* 12.7, pp. 624–626. ISSN: 1745-2473. DOI: [10.1038/nphys3784](https://doi.org/10.1038/nphys3784). URL: <http://www.nature.com/articles/nphys3784>.
- Levitov, L S and J Rhyner (1988). “Crystallography of quasicrystals ; application to icosahedral symmetry”. In: *J. Phys. France* 49, pp. 1835–1849. DOI: [10.1051/jphys:0198800490110183500](https://doi.org/10.1051/jphys:0198800490110183500). URL: <https://hal.archives-ouvertes.fr/jpa-00210865/document>.
- Mackay, Alan L. (1982). “Crystallography and the penrose pattern”. In: *Physica A: Statistical Mechanics and its Applications* 114.1-3, pp. 609–613. ISSN: 0378-4371. DOI: [10.1016/0378-4371\(82\)90359-4](https://doi.org/10.1016/0378-4371(82)90359-4). URL: <https://www.sciencedirect.com/science/article/pii/0378437182903594>.
- Rayleigh, Lord (1888). “XXVI. On the remarkable phenomenon of crystalline reflexion described by Prof. Stokes”. In: *The London, Edinburgh, and Dublin Philosophical Magazine and Journal of Science* 26.160, pp. 256–265. ISSN: 1941-5982. DOI: [10.1080/14786448808628259](https://doi.org/10.1080/14786448808628259). URL: <https://www.tandfonline.com/doi/full/10.1080/14786448808628259>.
- Rodriguez, Alejandro W. et al. (2008). “Computation and visualization of photonic quasicrystal spectra via Bloch’s theorem”. In: *Physical Review B* 77.10, p. 104201. ISSN: 1098-0121. DOI: [10.1103/PhysRevB.77.104201](https://doi.org/10.1103/PhysRevB.77.104201). URL: <https://link.aps.org/doi/10.1103/PhysRevB.77.104201>.
- Rostami, Ali and Samiye Matloub (2009). “BAND STRUCTURE AND DISPERSION PROPERTIES OF PHOTONIC QUASICRYSTALS”. In: *Progress In Electromagnetics Research M* 9, pp. 65–78. ISSN: 1937-8726. DOI: [10.2528/PIERM09091002](https://doi.org/10.2528/PIERM09091002). URL: <http://www.jpier.org/PIERM/pier.php?paper=09091002>.
- Russell, P. (2003). “Photonic Crystal Fibers”. In: *Science* 299.5605, pp. 358–362. ISSN: 00368075. DOI: [10.1126/science.1079280](https://doi.org/10.1126/science.1079280). URL: <http://www.ncbi.nlm.nih.gov/pubmed/12532007><http://www.sciencemag.org/cgi/doi/10.1126/science.1079280>.
- Senechal, Marjorie. (1995). *Quasicrystals and geometry*. Cambridge University Press, p. 286. ISBN: 0521575419. URL: <https://books.google.de/books/about/>

Quasicrystals and Geometry .html?id=LdQ8AAAAIAAJ&redir\_esc=y.

Shechtman, D. et al. (1984). “Metallic Phase with Long-Range Orientational Order and No Translational Symmetry”. In: *Physical Review Letters* 53.20, pp. 1951–1953. ISSN: 0031-9007. DOI: [10.1103/PhysRevLett.53.1951](https://doi.org/10.1103/PhysRevLett.53.1951). URL: <https://link.aps.org/doi/10.1103/PhysRevLett.53.1951>.

Wang, K. et al. (2003). “Photonic band gaps in quasicrystal-related approximant structures”. In: *Journal of Modern Optics* 50.13, pp. 2095–2105. ISSN: 0950-0340. DOI: [10.1080/09500340308235260](https://doi.org/10.1080/09500340308235260). URL: <http://www.tandfonline.com/doi/abs/10.1080/09500340308235260>.

Wolf, R.M. de and W. van Aalst (1972). “The four dimensional group of  $\gamma$ -Na<sub>2</sub>CO<sub>3</sub>”. In: *Acta Crystallogr. A* 28, S111.

Yablonovitch, Eli and Eli (1987). “Inhibited Spontaneous Emission in Solid-State Physics and Electronics”. In: *Physical Review Letters* 58.20, pp. 2059–2062. ISSN: 0031-9007. DOI: [10.1103/PhysRevLett.58.2059](https://doi.org/10.1103/PhysRevLett.58.2059). URL: <https://link.aps.org/doi/10.1103/PhysRevLett.58.2059>.